Design and Simulation of a Tactile Sensor for Fruit Ripeness Detection

Chiebuka T. Nnodim, *Member, IAENG,* Ahmed M. R. Fath El-Bab, Bernard W. Ikua, and Daniel N. Sila.

***Abstract*—Mechanical damages have been caused by the process of pressing mango fruits to check for it's ripeness. In order to reduce this damage, two varieties of mangoes namely Totapuri and Tommy Atkins were tested by an advanced universal testing machine (UTM). Each of these varieties had 5 samples of different ripeness levels to test for their elastic modulus. The mangoes were loaded radially and the results of the elastic modulus obtained, falls between 0.5MPa and 3.5MPa. This paper aims at presenting a detailed design procedure for developing a tactile sensor that can differentiate between different ripeness levels in mango fruit. The tactile sensor is based on two springs configuration, each of these springs having different stiffness. These design procedures were carried to achieve high sensitivity and linearity in the sensor output. The measuring range of the sensor was selected based on the modulus of elasticity of mango fruit chosen from the compression tests carried out on the mango fruit. The performance of the tactile sensor was studied by developing a finite element model using the ANSYS Mechanical ANSYS Parametric Design Language (APDL) software. The simulation results gotten from the performance of the tactile sensor shows that the sensor can differentiate between different mango fruits based on their elastic modulus within the specified range of the sensor.**

***Index Terms*—Elastic modulus, Mango fruit, simulation, Tactile sensor.**

I. Introduction

FRUITS are harvested when they are mature and hard in order to avoid perishing of during transportation from one location to another. These fruits are then stored until they get ripe and ready for consumption. Mango, which is the case study in this work is relatively cheap and affordable but they have some complexities in determining their ripeness. However, change in colour of these fruits does not guarantee their ripeness, in most cases, ripeness is determined by pressing the fruits to check if it is soft and this technique is not optimal because, in the process of pressing these fruits, it exposes the fruit to non-uniform ripeness and when the unripe part ripens, the already ripened part tends to spoil. This has an effect on the taste and quality of the fruits and mostly have led to wastage of these fruits. This has been an issue of concern and at the same time an issue of negligence.

Many researchers have carried out lots of work in fruit sorting and ripeness detection based on imaging system as in [1], [2], [3], based on electronic nose as in [4] and also based on the parameters affecting fruit quality as in [5], [6], [7]. Kunpeng et al [8] worked on Mechanical properties and compression damage simulation by finite element for kiwifruit, he found that the average elastic modulus of kiwi fruit on radial loading is $1.71MPa$. Alan et al [9] also carried out a mechanical characterization of mango fruit using compression tests to determine the elastic modulus of the two varieties of mangoes they worked with. from their results, the range of elastic modulus on radial of the mangoes they worked on is between $1MPa$ and $2.5MPa$. Accordingly, no work has been recorded in detection of fruit ripeness based on its elastic modulus and stiffness. Sensors which have been employed by many researchers in stiffness sensing of objects are tactile sensors.

Tactile sensors have a variety of industrial applications,including robotics[10], haptic devices[11], biomedical sensing[12], and polymer characterization[13]. A tactile sensor according to Lee et al[14], is a device or system that can characterize mechanical properties of the targeted object or of the contact between the sensor and the object. Tactile sensors for contact force measurement have been well documented, and a number of prototype sensors have been developed[15].

Different concepts have been applied in tactile sensor development for soft tissue stiffness measurement. However, the 2 tip configuration concept employed by [16] has an advantage of being independent of the applied displacement and force on the sensor. Fath El Bab et al. [16], [17] worked on softness of tissue compliance detection applying the two springs concept to differentiate soft tissues with different stiffness, they also showed that springs with cubic tip gives more stable output than springs with spherical tip. Fouly et al. [18], [19] modified the two springs concept to a three tip concept based on the fact that tissues have irregularities in their shape and developed a new tactile sensor that compensates for irregularities in the tissue shape to differentiate between tissues with different stiffness.

However, this paper aims to present a tactile sensor based on the concept of applying two springs with optimized spring stiffness to mango for ripeness detection. The range of measurement of the sensor is chosen based on the experiment conducted on the mango fruit. Subsequently, the parameters of the sensor are optimized, so as to increase sensitivity and linearity of the sensor output; and a finite element model is developed to make finite element analysis on the performance of the sensor with the designed parameters of the sensor with cubic tip.

II. Compression Tests on Mango

A. Test Materials and Methods

Five samples of Totapuri mango and Five samples of Tommy Atkins mango were being tested. These mangoes

Manuscript received June 27, 2019; revised July 21, 2019. This work was supported by the Pan African Union Scholarship and Japan International Cooperation Agency (JICA).

C. T. Nnodim is with the Department of Mechatronic Engineering, Pan African University, Institute for Basic Sciences, Technology and Innovation (e-mail: nnodimchiebuka.tim@gmail.com).

A. M. R. Fath EL-Bab is with the Department of Mechatronics and Robotics Engineering, Egypt-Japan University of Science and Technology.

B. W. Ikua is with the Department of Mechatronic Engineering, Jomo Kenyatta University of Agriculture and Technology.

D. N. Sila is with the Department of Food Science and Technology, Jomo Kenyatta University of Agriculture and Technology.

were selected so as to have different ripeness levels from ripe to unripe in order to have a wide range for the sensor. The fruits were loaded radially on a UTM and the fruits were compressed with a (30mm x 30mm x 70mm) compression plate. The speed of the compression test selected was 5mm/min. The radial height of the mangoes ranged from 65mm to 70mm which was measured by vernier calipers. The set up of the experiment is as shown in Fig.1 and the mangoes where compressed until failure as shown in Fig.2.

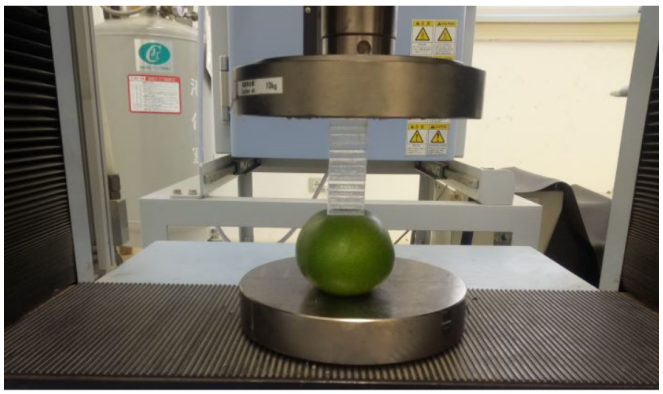

Fig. 1. Experimental Setup

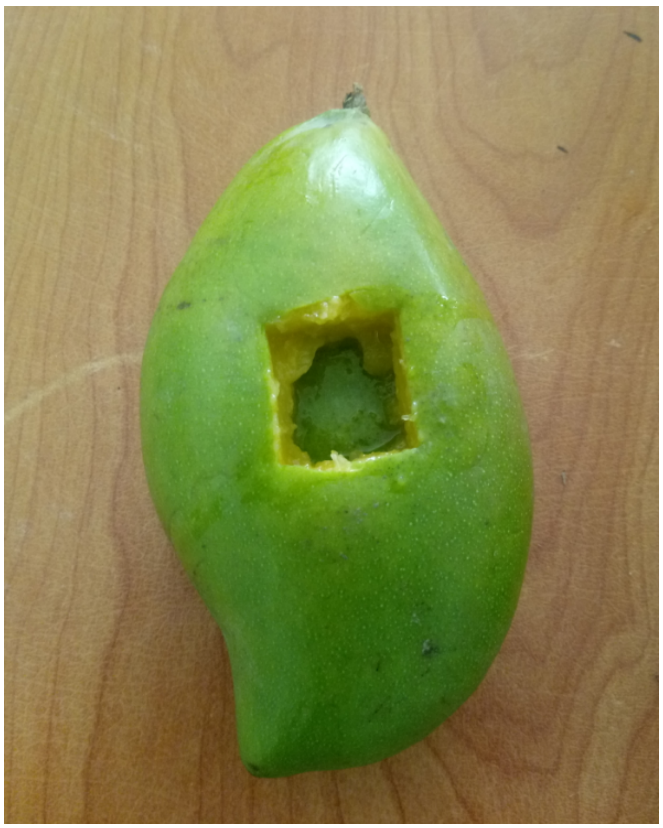

Fig. 2. Sample After Compression

The Force-displacement curve for each sample was generated from the TRAPEZIUM X software installed in the Pc which is connected to the Universal Testing machine (UTM). From the Force-displacement curve, the stress-strain curve for each sample was generated taking into consideration the radial height of the mangoes and the surface area of the compression plate. The stress-strain curve of the experiment is as shown in Figs.3, and 4. The values of the Elastic modulus was computed from the stress strain curves, and the values are shown in Table I.

TABLE I
ELASTIC MODULUS OF THE TESTED MANGOES

Sample	Elastic Modulus (MPa) for Totapuri Mango	Sample	Elastic Modulus (MPa) for Tommy Atkins Mango
Mango 1	3.23 ± 0.03	Mango 6	3.18 ± 0.15
Mango 2	1.78 ± 0.18	Mango 7	1.75 ± 0.14
Mango 3	1.1 ± 0.09	Mango 8	1.41 ± 0.15
Mango 4	1.0 ± 0.15	Mango 9	3.08 ± 0.08
Mango 5	2.42 ± 0.08	Mango 10	1.08 ± 0.27

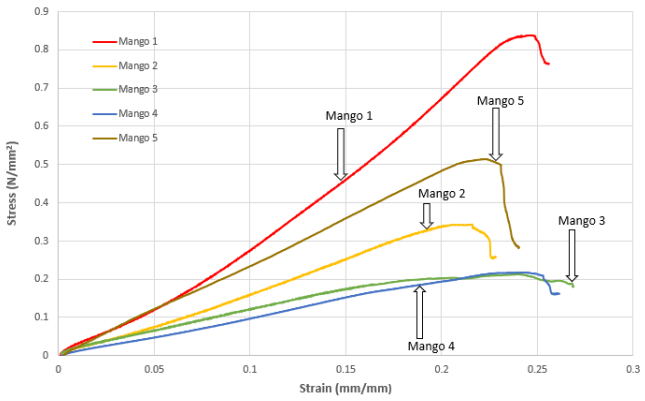

Fig. 3. Stress-strain curve for Totapuri Mango

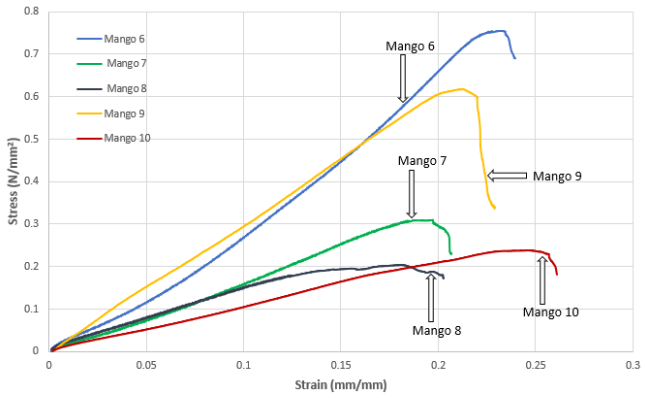

Fig. 4. Stress-strain curve for Tommy Atkins Mango

III. SENSOR DESIGN

A. Mathematical Model

The sensor design consists of two springs with stiffnesses (K_l) and (K_h) on the left and right hand respectively as shown in Fig.8. The mango stiffness (K_m) is modeled as an elastic spring [20]. (K_l) is the low stiffness spring while (K_h) is the high stiffness spring. As the sensor is pushed at a distance (x) to make contact with the mango, forces are generated on the low and high stiffness springs. These forces are (F_L) and (F_H) respectively. It can be seen in Fig.5 that (K_l) and (K_h) are in series with the mango spring (K_m); therefore, their equivalent stiffnesses (K_L) and (K_H) as shown in Fig.6 is mathematically shown in (1) and (2).

$$K_H = \frac{K_h K_m}{K_h + K_m} \tag{1}$$

ISBN: 978-988-14048-7-9
ISSN: 2078-0958 (Print); ISSN: 2078-0966 (Online)

$$K_L = \frac{K_l K_m}{K_l + K_m} \quad (2)$$

Furthermore, by measuring the ratio of the forces (P) i.e.

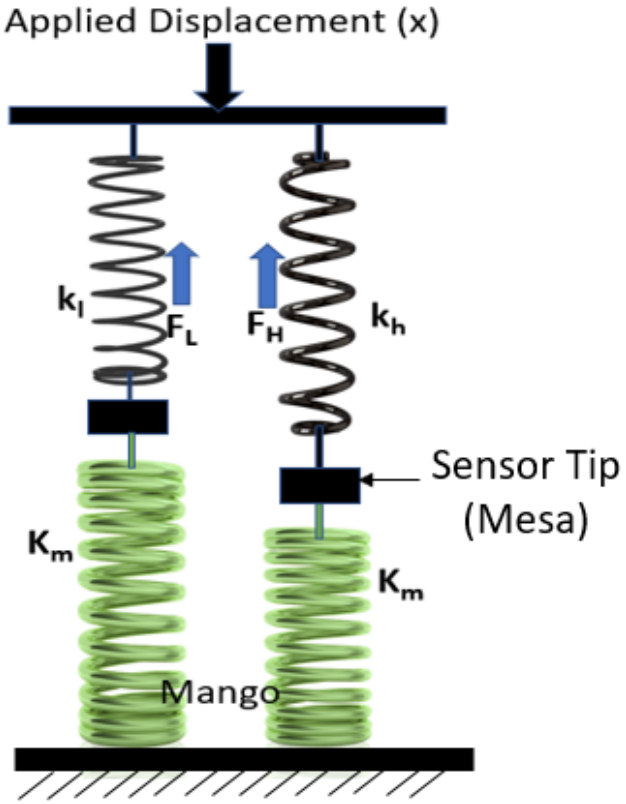

Fig. 5. Sensor Model

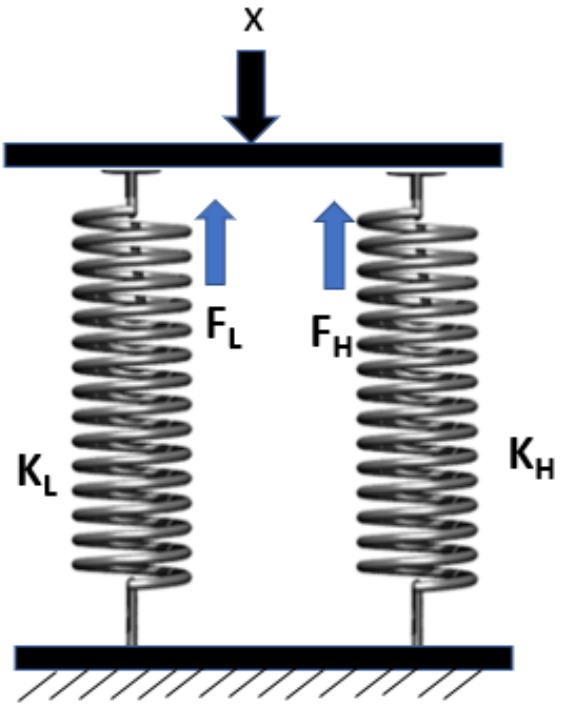

Fig. 6. Equivalent Model of the Sensor

the sensor output in (3) generated in the springs when pushed to the mango, the stiffness of the mango can be measured as shown in (4).

$$P = \frac{F_H}{F_L} = \frac{K_h(K_m + K_l)}{K_l(K_m + K_h)} \quad (3)$$

Where P is a dimensionless parameter.

$$K_m = \frac{K_h K_l(1 - P)}{PK_l - K_h} \quad (4)$$

B. Mango Fruit Stiffness Range

Hayes et al [21] provided a mathematical model based on indentation principle as shown in Fig. to calculate the stiffness of a soft object as a function of its elastic modulus as shown in (5).

$$E_m = \frac{(1 - \nu^2)F}{2rdC_k} \quad (5)$$

$$K_m = \frac{2rE_m C_k}{(1 - \nu^2)} \quad (6)$$

Where: F, ν, d, r, E_m, C_k and h are the applied force, Poisson's ratio of mango, the indentation depth, the indenter radius, the Elastic modulus of mango, the scaling factor and the radial height of the mango respectively. The indentation principle with a plain end indenter is as shown in Fig.7.

In order to determine the elastic modulus of mango, some researchers have carried out some work in order to achieve this. Alan et al [9], carried out mechanical characterization of mango fruit using compression tests on Keitt mango and Tommy Atkins mango at different stages of maturation, they found that the range of elastic modulus for both mangoes between $1MPa$ to $2.5MPa$ at a reducing order of ripeness. As mangoes matures (ripens), the mechanical properties reduces [6]. There are many studies on elastic modulus and Poisson's ratio of fruits and vegetables having their range of values. In the current work, mango is assumed to be isotropic and linear elastic especially when deformed slightly, its Poisson's ratio is assumed to be 0.3 and the maximum range of elastic modulus is $3.5MPa$ from the experiment of this work, which is equal to a stiffness value of $3850N/m$ according to (6). Also, the indenter is designed to be a cube with side length of $1mm$ and the radial height of the mango is $70mm$. However, the scaling factor C_k depends on ν, (r/h) and (d/h); Zhang et al [22] developed tables from a finite element analysis to estimate C_k, and obtained C_k = 1. Finally, from the experiment carried out in this work, the stiffness values will range from $0N/m$ to $3850N/m$ based on (6).

C. Sensor Parameters

The sensor parameters are the low stiffness sensor (K_l), the high stiffness sensor (K_h) and the force ratio (P). The maximum force ratio (P_{max}) can be calculated by defining (K_l) and (K_h) at maximum (K_m) in (3). However, doing that will increase the error in P due to crosstalk (interference) effect and cause a very large difference between (K_l) and (K_h). Fath El Bab et al [16], carried out a crosstalk effect analysis and found the P_{max} to be 5; thus, the selected P_{max} value in this work based on (3). As stated earlier, the relationship between P and k_m as in (3), is non linear when arbitrary values of K_l and K_h as shown in ; however a non linearity error analysis was done in order to get the desired

ISBN: 978-988-14048-7-9
ISSN: 2078-0958 (Print); ISSN: 2078-0966 (Online)

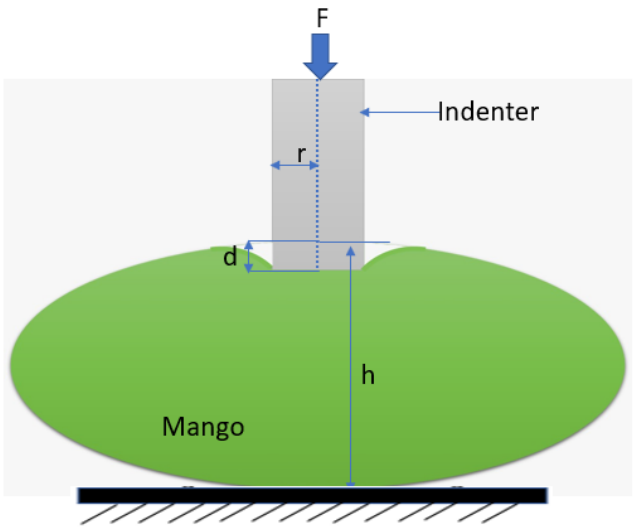

Fig. 7. Indentation Principle

K_l and K_h that gives a linear output. Fig.8 shows that the maximum non linearity occurs at the mid range of the mango stiffness. Therefore, the maximum nonlinearity error (NL)

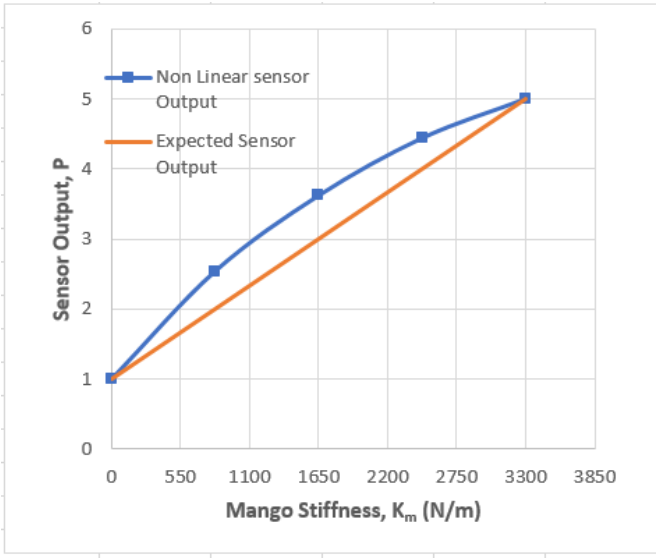

Fig. 8. Nonlinear and Expected Sensor Output Vs Mango Stiffness

from Fig.8,is represented mathematically in (7)

$$NL = \frac{m}{P_{max} - 1} = \frac{(P_{1925} - 1) - (P_{max} - 1)/2}{P_{max} - 1} \tag{7}$$

Where, P_{1925} is the sensor output at the mid-range of the mango stiffness designed, m is the distance between the maximum point of nonlinearity to the corresponding linear point as shown in Fig.8. Therefore, for P_{max} = 5, (7) becomes;

$$NL = \frac{P_{1925} - 3}{4} \tag{8}$$

Also from (3),

$$P_{1925} = \frac{K_h(1925 + K_l)}{K_l(1925 + K_h)} \tag{9}$$

The relationship between K_l and K_h at P_{max} from (3) becomes;

$$K_h = \frac{K_m P_{max}}{1 + (K_m/K_l) - P_{max}} = \frac{4812.5K_l}{962.5 - K_l} \tag{10}$$

Substituting (10) into (9), we get

$$P_{1925} = \frac{9625 + 5K_l}{1925 + 3K_l} \tag{11}$$

Subsequently, substituting (11) into (8),

$$NL = \frac{962.5 - K_l}{1925 + 3K_l} \tag{12}$$

Equation (12) shows the relationship between the between NL and K_l, which implies that NL is a function of change in K_l as shown in Fig.9. However, from Fig. 11, if a higher value of K_l is selected, then the value of K_h will be increased which will make the strain on the high stiffness sensor very low and this will consequently lead to a low output voltage.In this work, a nonlinearity error of 5% is assumed to be allowed, and this gives a value of $753N/m$ for K_l and $17300N/m$ for K_h. Having carefully selected our parameters, a 3-D Finite Element Analysis (FEA) was used to analyze the sensor performance of the proposed sensor in the next section.

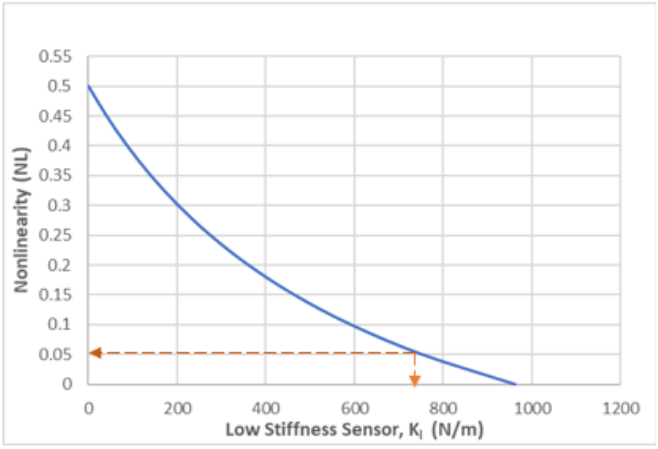

Fig. 9. Nonlinearity Versus the Low Sensor Stiffness, K_l (N/m)

IV. Finite Element Model and Analysis

The design parameters gotten in the previous section is used to build a Finite element model using ANSYS Mechanical APDL (ANSYS Parametric Design Language) software to analyze the sensor performance in this section.

A. Description of Model

The mango was constructed using a 3-D axisymmetric Finite element model, the mango was assumed to be isotropic, homogeneous, fixed below at its base, and linearly elastic with a Poisson's ratio of 0.3 with dimensions of $20mm$ x $12mm$ x $20mm$ as shown in Fig.10. Also the elastic modulus of the mango tested were $0.5MPa$, $1MPa$, $1.5MPa$, $2MPa$, $2.5MPa$ and $3MPa$ which equals $550N/m$, $1100N/m$, $1650N/m$, $2200N/m$, $2750N/m$ and $3300N/m$ respectively according to Hayes et al. model [21]. The distance between the sensor tips is $8mm$, this is narrow

ISBN: 978-988-14048-7-9
ISSN: 2078-0958 (Print); ISSN: 2078-0966 (Online)

enough to assume that the surface of contact is flat. The sensor tips which is a rigid body attached to the spring during pushing is cubic with a side length $1mm$,the sensor tip in the model is at a distance $0.5mm$ above the fruit. The contact of the sensor tip with the mango was built with CONTA174 and TARGE170 elements located on its boundary. The sensors are the two springs of COMBIN14 elements, which represents the low stiffness sensor (K_l)=$753N/m$ on the left and the high stiffness sensor (K_h)= $17300N/m$ on the right as shown in Fig.10. MESH200 elements was applied on the surface area of the mango with the contact zones highly refined. The applied displacement into the mango is $0.6mm$.

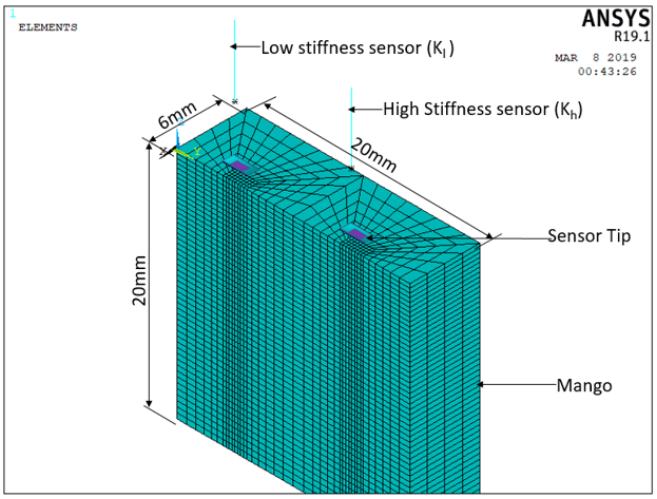

Fig. 10. A 3-D Axisymmetric Finite Element Model

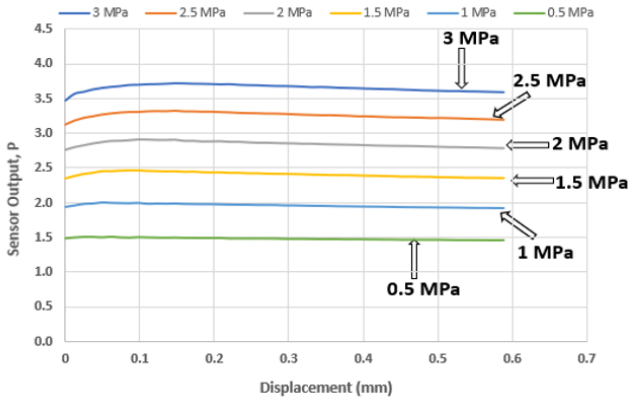

Fig. 11. Sensor Output, P Versus Displacement, x (mm)

V. Results and Discussion

A. Compression Tests on Mango

Figs. 3 and 4 show stress-strain curves of the Totapuri mango and Tommy Atkins mango, the experiment was able to estimate the Elastic modulus of each sample based on its level of maturation as shown in Table I. It was deduced that the stiffest mangoes amongst the samples tested had the highest elastic modulus, and then the softest of them had the least elastic modulus. This is to say that as ripeness (maturation) increases, the mechanical properties like elastic modulus and stiffness reduces. The experiment also showed that the elastic modulus of different maturation levels of mango falls in the range of $0.5MPa$ to $3.5MPa$.From the experiments conducted in this work, the stiffest mangoes had an elastic modulus greater than $3MPa$; to this effect, the maximum range of our sensor was selected to be $3.5MPa$.

B. Sensor Output

Elastic modulus of $0.5MPa$, $1MPa$, $1.5MPa$, $2MPa$, $2.5MPa$ and $3MPa$ which equals $550N/m$, $1100N/m$, $1650N/m$, $2200N/m$, $2750N/m$ and $3300N/m$ respectively according to Hayes et al. model [21] were simulated by the finite element analysis. The results as shown in Fig. 11 shows that the sensor was able to differentiate between the different stiffnesses of the mango and the output readings where stable along the displacement of 0.6mm .

Finally, from the results of the simulation, a macro tactile sensor with sensor stiffness values K_l = $753N/m$ and K_h = $17300N/m$ will be fabricated in the coming days.

VI. Conclusion

This paper has presented the simulation of a tactile sensor for mango ripeness measurement which is based on the principle of applying two springs with different stiffness properly designed. The parameters of the sensors were optimized to give high sensitivity and linearity of its output. The sensor measuring range is up to $3.5MPa$ so as to cover a wider range of fruits in this class. The performance of the sensor was studied by carrying out a Finite element analysis on the model. The mango was modeled as a cube of $20mm$ x $12mm$ x $20mm$, having a Poisson's ratio of 0.3 and elastic modulus varying from $0.5MPa$ to $3.5MPa$, which is equal to stiffness of $550N/m$ to $3850N/m$ respectively.

Finally, the Finite element analysis on the performance of the sensor demonstrated that the sensor is able to differentiate different mangoes based on their elastic modulus in the designed range up to $3.5MPa$. Also the sensor output P is independent on the displacement (pushing distance), however a linear output was achieved.

Acknowledgment

This work is supported by Japan International Cooperation Agency (JICA) through the Pan African University Institute for Basic Sciences, Technology and Innovation (PAUSTI). The authors would like to thank Egypt-Japan University of Science and Technology (E-JUST) for enabling the authors use her research facilities and resources to accomplish this work.

References

[1] E. H. Yossy, J. Pranata, T. Wijaya, H. Hermawan, and W. Budiharto, "Mango Fruit Sortation System using Neural Network and Computer Vision," *Procedia Computer Science*, vol. 116, pp. 596–603, 2017.
[2] M. Shiddiq, Fitmawati, R. Anjasmara, N. Sari, and Hefniati, "Ripeness detection simulation of oil palm fruit bunches using laser-based imaging system," *AIP Conference Proceedings*, vol. 1801, 2017.
[3] I. Sa, Z. Ge, F. Dayoub, B. Upcroft, T. Perez, and C. McCool, "Deepfruits: A fruit detection system using deep neural networks," *Sensors (Switzerland)*, vol. 16, no. 8, 2016.
[4] S. M. Praveena, "Evaluation of Fruit Ripeness Using Electronic Nose," *International Journal of Advanced Information Science and Technology (IJAIST)*, vol. Vol.6, no. June, 2017.

ISBN: 978-988-14048-7-9
ISSN: 2078-0958 (Print); ISSN: 2078-0966 (Online)

[5] V. G. Verzhuk, S. V. Murashev, and a. Y. Belova, "Determination of tissue elasticity of apple, pear, and quince fruits for predicting losses during cold storage," *Russian Agricultural Sciences*, vol. 38, no. 4, pp. 272–274, 2012.
[6] B. Jarimopas and U. Kitthawee, "Firmness properties of mangoes," *International Journal of Food Properties*, vol. 10, no. 4, pp. 899–909, 2007.
[7] S. Cárdenas-Pérez, J. J. Chanona-Pérez, N. Güemes-Vera, J. Cybulska, M. Szymanska-Chargot, M. Chylinska, A. Kozioł, D. Gawkowska, P. M. Pieczywek, and A. Zdunek, "Structural, mechanical and enzymatic study of pectin and cellulose during mango ripening," *Carbohydrate Polymers*, vol. 196, no. January 2019, pp. 313–321, 2018.
[8] T. Kunpeng, S. Cheng, L. Xianwang, H. Jicheng, C. Qiaomin, Z. Bin, K. P. Tian, C. Shen, X. W. Li, J. C. Huang, Q. M. Chen, and B. Zhang, "Mechanical properties and compression damage simulation by finite element for kiwifruit," *International Agricultural Engineering Journal*, vol. 26, no. 4, pp. 193–203, 2017.
[9] A. Dantas, R. Barbosa, A. F. Neto, and L. I. N. Hernández, "Mango mechanical compression tests.pdf," *Revista de Ciencias Agrarias*, vol. 40, no. 2, pp. 405–410, 2017.
[10] K. Suwanratchatamanee, M. Matsumoto, and S. Hashimoto, "Haptic sensing foot system for humanoid robot and ground recognition with one-leg balance," *IEEE Transactions on Industrial Electronics*, vol. 58, no. 8, pp. 3174–3186, 2011.
[11] I. Peterlík and J. Filipovič, "Distributed construction of configuration spaces for real-time haptic deformation modeling," *IEEE Transactions on Industrial Electronics*, vol. 58, no. 8, pp. 3205–3212, 2011.
[12] R. Aoyagi and T. Yoshida, "Frequency equations of an ultrasonic vibrator for the elastic sensor using a contact impedance method," *Japanese Journal of Applied Physics, Part 1: Regular Papers and Short Notes and Review Papers*, vol. 43, no. 5 B, pp. 3204–3209, 2004.
[13] A. M. Sánchez, R. Prieto, M. Laso, and T. Riesgo, "A piezoelectric minirheometer for measuring the viscosity of polymer microsamples," *IEEE Transactions on Industrial Electronics*, vol. 55, no. 1, pp. 427–436, 2008.
[14] M. Lee and H. Nicholls, "Review Article Tactile sensing for mechatronicsa state of the art survey," *Mechatronics*, vol. 9, no. 1, pp. 1–31, 1999.
[15] R. Cecchi, M. Verotti, R. Capata, A. M. Dochshanov, G. B. Broggiato, R. Crescenzi, M. Balucani, S. Natali, G. Razzano, F. Lucchese, A. Bagolini, P. Bellutti, E. Sciubba, and N. P. Belfiore, "Development of micro-grippers for tissue and cell manipulation with direct morphological comparison," *Micromachines*, vol. 6, no. 11, pp. 1710–1728, 2015.
[16] A. M. R. F. El Bab, T. Tamura, K. Sugano, T. Tsuchiya, O. Tabata, M. E. H. Eltaib, and M. M. Sallam, "Design and simulation of a tactile sensor for soft-tissue compliance detection," *IEEJ Transactions on Sensors and Micromachines*, vol. 128, no. 5, pp. 186–192, 2008.
[17] A. Fath El-Bab, M. Eltaib, M. Sallam, and O. Tabata, "Tactile sensor for compliance detection," *Sensors and Materials*, vol. 19, no. 3, pp. 165–177, 2007.
[18] A. Fouly, M. N. Nasr, A. M. Fath El Bab, and A. A. Abouelsoud, "Design and modeling of micro tactile sensor with three contact tips for self-compensation of contact error in soft tissue elasticity measurement," *IEEJ Transactions on Electrical and Electronic Engineering*, vol. 10, pp. S144–S150, 2015.
[19] A. Fouly, A. M. FathEl-Bab, M. N. Nasr, and A. A. Abouelsoud, "Modeling and experimental testing of three-tip configuration tactile sensor for compensating the error due to soft tissue surface irregularities during stiffness detection," *Measurement: Journal of the International Measurement Confederation*, vol. 98, pp. 112–122, 2017.
[20] J. Engel, J. Chen, Z. Fan, and C. Liu, "Polymer micromachined multimodal tactile sensors," *Sensors and Actuators, A: Physical*, vol. 117, no. 1, pp. 50–61, 2005.
[21] W. C. Hayes, L. M. Keer, G. Herrmann, and L. F. Mockros, "A mathematical analysis for indentation tests of articular cartilage," *Journal of Biomechanics*, vol. 5, no. 5, pp. 541–551, 1972.
[22] M. Zhang, Y. P. Zheng, and A. F. T. Mak, "Estimating the effective Young's modulus of soft tissues from indentation tests - Nonlinear finite element analysis of effects of friction and large deformation," *Medical Engineering and Physics*, vol. 19, no. 6, pp. 512–517, 1997.

ISBN: 978-988-14048-7-9
ISSN: 2078-0958 (Print); ISSN: 2078-0966 (Online)